Available online at www.sciencedirect.com
ScienceDirect
Ceramics International 35 (2009) 2563–2569
CERAMICS INTERNATIONAL
www.elsevier.com/locate/ceramint

Template-directed hydrothermal synthesis of dandelion-like hydroxyapatite in the presence of cetyltrimethylammonium bromide and polyethylene glycol

Mehrnaz Salarian [a,*], Mehran Solati-Hashjin [b], Seyedeh Sara Shafiei [b], Reza Salarian [c], Ziarat Ali Nemati [d]

[a] School of Materials Engineering, Science and Research Branch, Islamic Azad University, Tehran, Iran
[b] Biomaterial Group, Faculty of Biomedical Engineering, Amirkabir University of Technology, Tehran, Iran
[c] Maziar University, School of Engineering, Mazandaran, Noor, Iran
[d] School of Materials Science and Engineering, Sharif University of Technology, Tehran, Iran

Received 18 August 2008; received in revised form 3 September 2008; accepted 2 February 2009
Available online 6 May 2009

Abstract

A template-directed synthetic method, using surfactant cetyltrimethylammonium bromide (CTAB) as a template and co-surfactant polyethylene glycol (PEG600) as a co-template under hydrothermal conditions, has been applied to obtain dandelion-like HAp. The morphology, size, crystalline phase, chemical composition, physical characteristics, and thermal behavior of the product were characterized by scanning electron microscopy (SEM), transmission electron microscopy (TEM), X-ray powder diffraction (XRD), Fourier ransform infrared spectroscopy (FTIR), induced coupled plasma spectroscopy (ICP), BET (Brunauer, Emmett, and Teller) method, and simultaneous thermal analysis (STA). SEM and TEM observations showed in the presence of CTAB and a certain concentration of PEG600 (30%) HAp crystals have a uniform dandelion-like morphology with a diameter of about 80–150 nm and aspect ratio of about 20 for each tooth. Dandelion-like HAp crystals have a high surface area of 88 $m^2\ g^{-1}$ showing potential applications. The template action of CTAB and co-template action of PEG600 are also discussed.

Keywords: Cetyltrimethylammonium bromide; Polyethylene glycol; Hydroxyapatite; Dandelion-like

1. Introduction

Hydroxyapatite (denoted as HAp), $Ca_{10}(PO_4)_6(OH)_2$, has been applied to medical fields such as reconstructive and prosthetic materials for bone and tooth owing to its excellent biocompatibility, bioactivity, high osteo-conductivity, and/or osteo-inductivity [1–3]. It can also find applications in other fields of industrial or technological interest as be used as catalyst in chromatography or gas sensor, water purification, fertilizers production, and drug carrier [4].

Characteristics of HAp such as osteo-conductivity, bioactivity, biocompatibility, solubility, sinterability, castability, fracture toughness, and adsorption can be tailored over wide ranges by controlling its crystal morphology [5–7]. Therefore, it is of great importance to develop HAp synthesis methods having focused on the precise control of the crystal morphology.

HAp can be synthesized by many chemical-processing routes such as solid-state reaction [8], co-precipitation [9], and hydrothermal technique [10]. The hydrothermal technique usually results in HAp powders with a high degree of crystallinity and a Ca/P ratio close to the stoichiometric value. However, the obtained powders are usual in agglomeration, and the size distribution is in the wide range [11]. A newly developed hydrothermal technique is template-directed hydrothermal method. Template-directed synthesis, an important synthetic strategy, is widely applied to control inorganic crystal morphology by adding organic ligands, additives, or templates [12–14]. A significant number of studies have focused on the synthesis of needle-like and rod-like HAp using cationic surfactant cetyltrimethylammonium bromide, which serves as a versatile soft template in HAp crystallization system [3,11,15–18]; Chaofan Qiu (2007) has reported

* Corresponding author. Tel.: +98 21 77829564; fax: +98 21 77829564.
E-mail address: mehrnazsalarian@gmail.com (M. Salarian).

0272-8842/$36.00
doi:10.1016/j.ceramint.2009.02.031

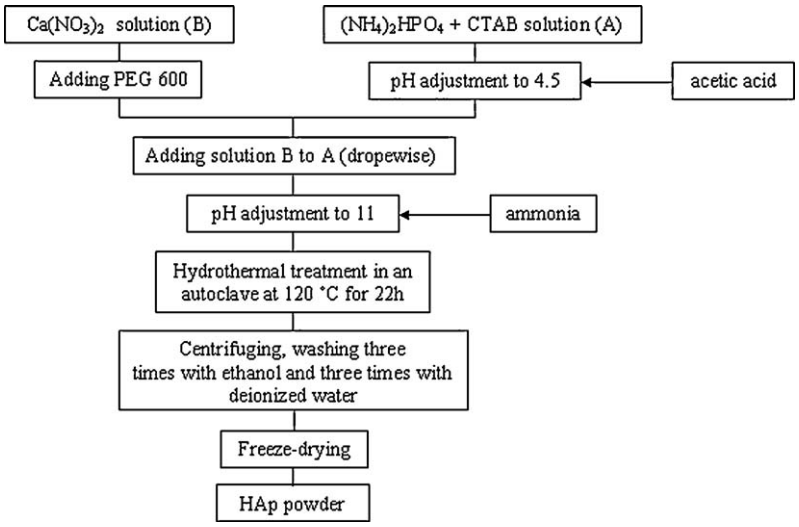

Fig. 1. The process flowchart for synthesis of dandelion-like HAp.

biomimetic synthesis of spherical nanometer HAp in the presence of polyethylene glycol 6000 [7]. However, surfactants CTAB and PEG have seldom been used simultaneously. Only once did Yingkai Liu (2004) synthesize HAp nano-rods by a precipitating calcium chloride and sodium phosphate using surfactant CTAB and co-surfactant polyethylene glycol 400 together [19]. In the present work, we conducted the hydrothermal synthesis of dandelion-like HAp in the presence of both CTAB and PEG600 as regulators of nucleation and crystal growth under hydrothermal conditions, and put the emphasis on the SEM and TEM morphology characterization of the HAp crystals.

Dandelion-like HAp crystals exhibit especial surface characteristics, and have a high surface area; thus, this morphology may open a new window for potential applications of HAp in the fields of catalyst, medication, photoelectric materials, chemical engineering, and environment engineering.

2. Experimental

2.1. Chemicals

Calcium nitrate tetrahydrate ($Ca(NO_3)_2{\cdot}4H_2O$) (Merck Prolabo 22 384.298), diammonium hydrogen phosphate ($(NH_4)_2HPO_4$) (Merck Prolabo 21 306.293), CTAB (Merck 102342), and PEG600 (Merck 807486) were used as starting materials. All chemicals were analytical grade and used with no further purification. The reactant molar ratio of Ca^{2+}/PO_4^{3-} was kept at 1.67 (stoichiometric ratio of HAp).

2.2. Preparation of the samples

First, 0.03 mole of $(NH_4)_2HPO_4$ and 0.021 mole of CTAB were dissolved completely in 125 ml of deionized water. This solution was stirred with a magnetic stirrer for 30 min to ensure that the cooperative interaction and self-assembly process were completed. Second, the pH value was adjusted to 4.5 by adding pure acetic acid. Next, 0.05 mole of $Ca(NO_3)_2.4H_2O$ was dissolved in 175 ml of deionized water, and PEG600 with different concentrations of 10%, 20%, and 30% was added to the solution under constant stirring for 30 min. Then, the mixed solution of $Ca(NO_3)_2{\cdot}4H_2O$ and PEG600 was added to the latter dropwise under continuous magnetic stirring in air. Finally, the pH value of reaction solution was adjusted to 11 using ammonia. The final milky suspension was transferred to a stainless steel autoclave; sealed tightly, and hydrothermally treated in an oven at 120 °C for 22 h. The resultant precipitates were separated from the suspension by centrifuging, washed three times with ethanol and three times with deionized water to remove the residual CTAB and PEG600, and freeze-dried to yield white powder. The flowchart for synthesis of dandelion-like HAp was the following as Fig. 1.

2.3. Characterization of the samples

The morphology and size of HAp particles were investigated by a XL30 Philips scanning electron microscopy (SEM) and a Philips EM208 transmission electron microscopy (TEM). The powders for SEM analysis were prepared by sprinkling the dried HAp onto one side of a double adhesive tape, which was stuck to an aluminum stub. The stub was then gold coated using EMITECH K450X (England) to a thickness of 20–30 nm, and examined with an accelerating voltage of 20 kV. The TEM sample was separated in an ethanol solution using ultrasonic vibration; then, picked up with the TEM copper grids coated with amorphous carbon film for TEM examinations.

Phase composition of the product was identified using the XRD pattern recorded by a D4 Bruker X-ray diffractometer system with a monochromatic Cu Kα radiation (λ = 1.5406 Å) over the 2θ range of 8–70° at a scan rate of 1° per minute in Guiner geometry. The operation voltage and current were 40 kV and 30 mA, respectively. To identify the functional groups, FT-IR spectrum was obtained on a Bruker IFS 48 spectrometer. The potassium bromide (KBr) disk technique was used for the analysis using 2 mg of HAp powder compacted with 200 mg of KBr under a hydraulic pressure. The spectrum

was recorded in the 4000–400 cm^{-1} region with 2 cm^{-1} resolution averaging 100 scans. The thermal behavior of the product was studied using TGA/DTA (STA; Polymer Laboratories PL-STA 1640) between room temperature to 1200 °C at a heating rate of 10 °C/min. The specific surface area of the product was calculated from the application of the BET equation to nitrogen adsorption isotherms obtained with a Micromeritics, Gemini 2375 surface area analyzer (USA) after calcinations at 400 °C for 30 min and degassing under vacuum at 200 °C. The calcium and phosphorus contents were determined by an inductively coupled plasma atomic emission spectrometer (ICP-AES, ARL 3410) by first dissolving in 2 mole dm^{-3} HNO_3 solution.

3. Results

3.1. SEM and TEM observations of the samples

To screen the influence of surfactants on the morphology of HAp particles, the synthesis process was conducted in the absence of both CTAB and PEG, in the presence of CTAB and absence of PEG, and in the presence of both CTAB and PEG with different concentrations of 10%, 20%, and 30%, and SEM was employed to characterize the morphology of the resultants. Fig. 2A shows the SEM micrograph of the sample synthesized in the absence of CTAB and PEG. As can be seen, in the absence of both surfactants HAp particles are spherical with diameter of about 50–100 nm. In addition, in the presence of CTAB and absence of PEG HAp particles have rod-like morphology with a typical diameter of about 50–120 nm and an average aspect ratio of about 4–6 shown in the Fig. 2B. In the presence of CTAB and PEG with concentration of 10%, the particles are too much thinner and longer with an aspect ratio of about 15–20 and a typical diameter of about 40–80 (Fig. 2C). Fig. 2D is the SEM micrograph of the sample synthesized in the presence of CTAB and PEG with concentration of 20%, and the HAp flakes are obviously observed in the sample. On the other hand, with increasing the PEG concentration to 30%, HAp crystals have a uniform dandelion-like morphology with an average diameter of about 80–150 nm and aspect ratio of about 20 for each tooth, illustrated in the Figs. 3 and 4, respectively.

3.2. XRD analysis of the product

The typical XRD pattern of the dandelion-like HAp is shown in the Fig. 5. As can be seen, all the diffraction peaks could be perfectly indexed to the standard pattern reported by the Joint Committee on Powder Diffraction Standards (JCPDS) for hexagonal HAp (file no: 09-432) represented by filled triangles. No characteristic peaks of impurities are detected in the pattern, which indicates that the product is pure HAp. There is also a sign of directional growth in the XRD pattern. In HAp standard

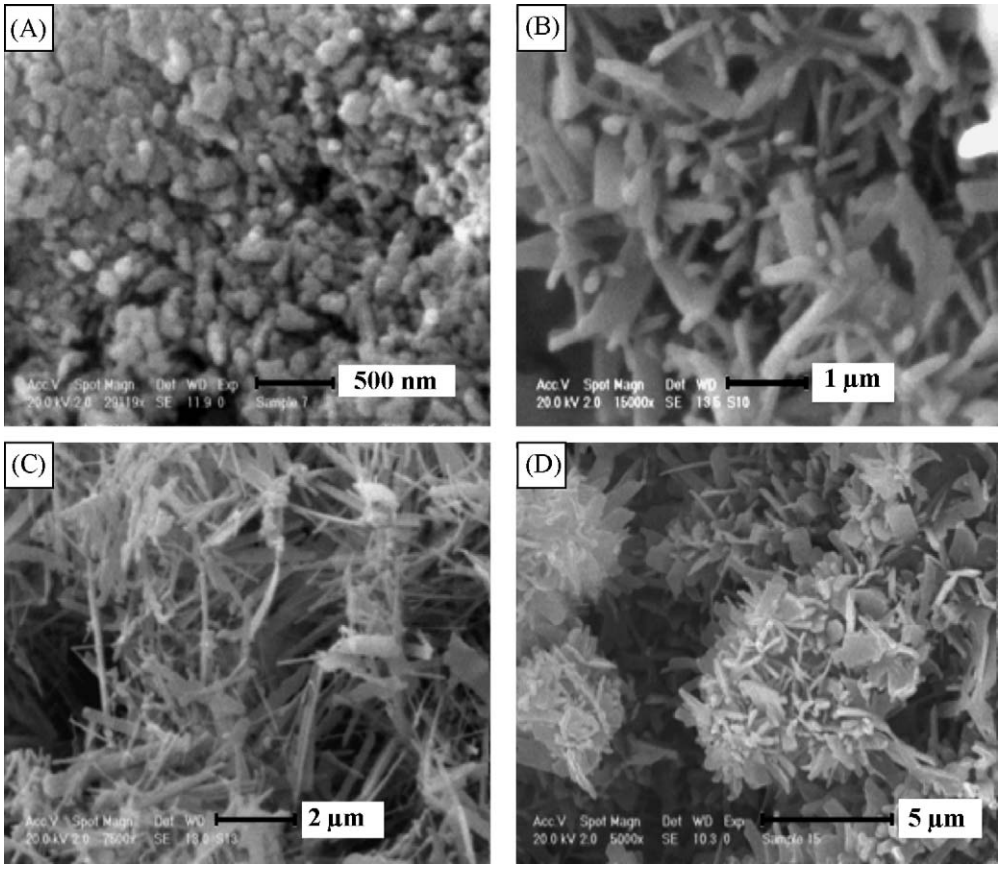

Fig. 2. The typical SEM micrographs of HAp samples synthesized in the absence of CTAB and PEG (A), in the presence of CTAB and absence of PEG (B), in the presence of CTAB and PEG with concentration of 10% (C), and in the presence of CTAB and PEG with concentration of 20% (D).

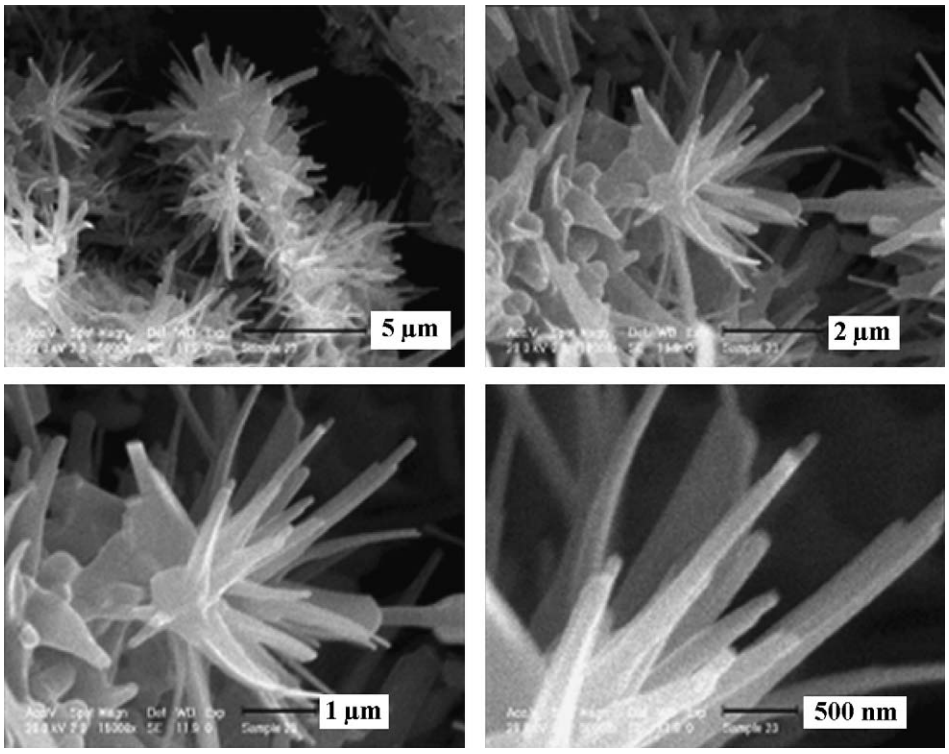

Fig. 3. The typical SEM micrograph of dandelion-like HAp.

pattern, the intensity of diffracted X-ray relating to (2 1 1) and (0 0 2) planes are assumed to be 100 and 40 units, respectively. Thus, the $I_{(2\ 1\ 1)}/I_{(0\ 0\ 2)}$ is equal to 2.5. In our sample diffraction peak of (0 0 2) is too sharp, and its relative intensity is far more than standard ($I_{(2\ 1\ 1)}/I_{(0\ 0\ 2)}$ is equal to 1.9). It indicates that the (0 0 2) plane is more full-grown; in other words, HAp dandelions are oriented to grow up along *c* axis.

3.3. FT-IR analysis of the product

Fig. 6 illustrates the typical FT-IR spectrum of the dandelion-like HAp. Absorption peaks at 882 and 1460 cm^{-1} are assigned to carbonate ions [20,21] which reveal that a certain level of carbonate substitution has taken place in the product. The carbonate ions may come from a reaction between atmospheric carbon dioxide and solution during the synthesis process. The characteristic bands for PO_4^{3-} appeared at 471.2 (υ_2 PO_4^{3-} [22]), 565 and 602.7 (υ_4 PO_4^{3-} [23]), 962 (υ_1 PO_4^{3-} [4]), 1031 and 1095 cm^{-1} (υ_3 PO_4^{3-} [24]). The two medium sharp peaks at 633 and 3570 cm^{-1} are attributed to viberational OH^- [19] and structural OH^- [23], respectively, which indicates the high crystallinity of the product as a result of hydrothermal treatment. The medium band at 1633 cm^{-1} is assigned to adsorbed water [19], and the broad band at 3428 cm^{-1} may come from lattice H_2O since this band exists in the range of 3550–3200 cm^{-1} for hydrated H_2O [11].

Fig. 4. The typical TEM micrograph of dandelion-like HAp.

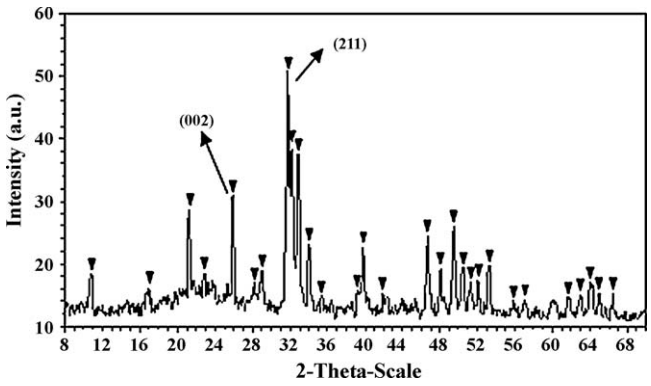

Fig. 5. The typical XRD diffraction pattern of dandelion-like HAp.

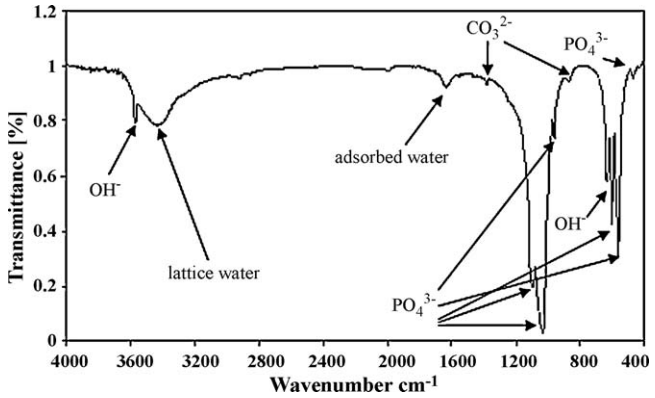

Fig. 6. The typical FT-IR spectrum of dandelion-like HAp.

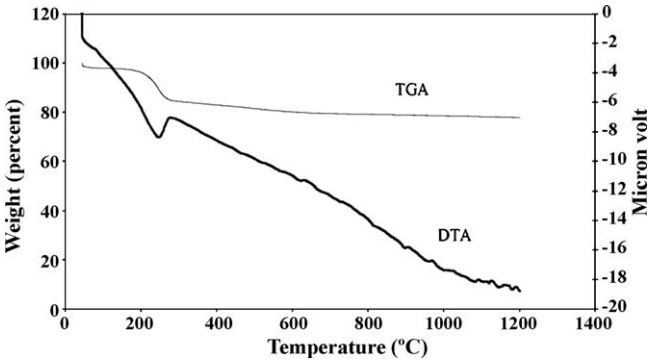

Fig. 7. The typical DTA and TGA curves of the HAp powder synthesized in the presence of CTAB and PEG with concentration of 30%.

3.4. Thermal analysis of the product

The differential thermal analysis (DTA) and thermogravimetric analysis TGA (STA: Simultaneous thermal analysis) curves of the HAp powder synthesized in the presence of CTAB and PEG with concentration of 30% are illustrated in Fig. 7.

The first endothermic trend took place between 90–295 °C with a peak at 250 °C, which corresponds to the dehydration and the loss of physically adsorbed water molecules of the HAp powder. The weight loss in this region is about 16%. No other endothermic and exothermic peaks were detected in the range of 296–1200 °C except a weight loss of 6% observed at the TGA curve in the temperature range, which is assumed to be the result of gradual dehydroxylation of HAp powder. This can be explained by the following reaction [20]:

$$Ca_{10}(PO_4)_6(OH)_2 \rightarrow Ca_{10}(PO_4)_6(OH)_{2-2x}O_x + xH_2O$$

3.5. Physical characteristics and chemical composition of the product

The physical characteristics and chemical composition of the dandelion-like HAp are shown in the Table 1. We can see from the Table that dandelion-like HAp benefits from high specific surface area (88 $m^2\ g^{-1}$). The Ca/P molar ratio in the Table is a direct measurement from the ICP analysis. From the Table, dandelion-like HAp has a higher Ca/P value than that of stoichiometric hydroxyapatite (1.67), which reflects the partial replacement of phosphate ions in the crystal lattice by carbonate. This result would mean that the product is not a non-substituted HAp, and the proposed chemical formula for the carbonate-substituted HAp is $Ca_{10-x/2}(PO_4)_{6-x}(CO_3)_x(OH)_2$. In the Table, carbonate content is evaluated by x value, which is determined by fitting *Ca/P* value to the above chemical formula, according to the following equations:

$$x = \frac{10 - 6 \times (Ca/P)}{0.5 - (Ca/P)} \quad (1)$$

Carbonate content can be calculated from the Eq. (2);

$$\text{Carbonate}[\text{Wt}\%] = \frac{M_{Co_3^{2-}} \times x}{M_{\text{CHAp}}} \quad (2)$$

where $M_{Co_3^{2-}}$ is the weight of carbonate ion, and M_{CHAP} is determined by fitting the x value calculated from Eq. (1) to the chemical formula of carbonate-substituted HAp.

4. Discussion

Effect of CTAB in HAp crystallization system is thought to be able to act as a soft template with the template action resulting in epitaxial growth of the product [4,19]. CTAB is a cationic surfactant, and its critical micelle concentration (CMC) is 0.03% (0.9–1.0 mM) [11]. Above CMC, a transition from spherical micelles to rod-like micelles occurs, and the size of micelles increases with the increase of CTAB concentration [11]. Micellar growth to rods can be considered to arise from two mechanisms. In one, there is an internal driving force to form large aggregates with another geometry. In another, micellar growth is induced by intermicelle repulsions to allow a better packing of the micelles. This will occur at high concentrations when the micelles come in direct close contact. Furthermore, PEG is a non-ionic surfactant and able to act as a co-template. Among the common water-soluble polymers, PEG is one of the most flexible polymers in an aqueous medium because of the flexible ether linkages in its backbone and the absence of bulky side groups. Thus, it is sterically less hindered in the aqueous medium [19].

Table 1
The physical characteristics and chemical composition of the dandelion-like HAp.

Sample	Ca [wt%]	P [wt%]	Ca/P Molar ratio	CO_3^{2-} [wt%]	Specific surface area ($m^2\ g^{-1}$)
Dandelion-like HAp	23.45	10.55	1.72	1.59	88

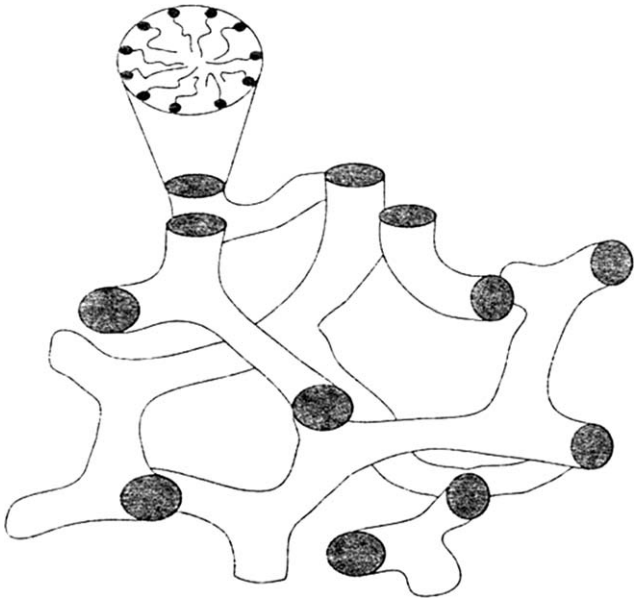

Fig. 8. Branched micelles.

Generally, there are two alternative pictures of mixed polymer-surfactant systems, one describing the interaction in terms of an association or binding of the surfactant to the polymer and one in terms of a micellization of surfactant on or in vicinity of the polymer chain. For polymers with hydrophobic groups the binding approach is preferred, while for polymers with hydrophilic groups such as PEG the micelle formation picture has distinct advantages. There is a close similarity between a polymer-induced micellization and the micellization of the surfactant alone; indeed, PEG, which is located in the outer part of the micelles, tends to strongly induce the micellar growth. In this case, the micelles creep like a snake through tubes in a porous structure given by the other micelles, so the viscosity increases very strongly with both micelle size and polymer concentration. Under certain conditions, such as a very high concentration (30%), the linear growth may lead to branched micelles which are completely connected (Fig. 8). In fact, another way to solve the problem of too strong crowding of the micelles is a structural transition into an ordered phase, so the concept of distinct micelles loses its meaning.

Moreover, in an aqueous system CTAB would ionize completely, and result in a cation with tetrahedral structure. The phosphate anion has also a tetrahedral structure [4,19]. By the charge and stereochemistry complementarily, a process called molecule recognition could be realized at the inorganic/organic interface. Thus, CTAB can be well incorporated to the phosphate anion [16]. When Ca^{2+} solution is added into PO_4^{3-} solution, $Ca_9(PO_4)_6$ is formed on the micellar surface of branched micelles. During the hydrothermal stage, CTAB-HAp complexes are formed, and they coalesce to form dandelion-like structures. In other words, the micelles act as nucleating sites for the growth of HAp crystals [4]. Therefore, the template and co-template action endow the surfactants with the capability to control the crystallization and growth processes.

5. Conclusion

In summary, dandelion-like hydroxyapatite showing potential applications has been successfully synthesized using template and co-template. XRD analysis confirmed that longitude direction of dandelions is [0 0 2]. FT-IR analysis proved that the product is CHAp although this is not shown by the XRD analysis. Since carbonated HAp seems to be a promising material for bioresorbable bone substitution due to the similarity to the composition of biological hydroxyapatite in natural bone, the CHAp particles obtained in this study are expected to demonstrate excellent bioactivity. Moreover, dandelion-like HAp shows a high specific surface area, confirmed by BET analysis. It will open a bright window for far-ranging applications.

Acknowledgements

The authors wish to thank Prof. F. Moztarzadeh for his support and companionship.

References

[1] S.F. Hulber, J.C. Bokros, L.L. Hench, J. Wilson, G. Heimke, Ceramics in Clinical Applications: Past, Present and Future, in: P. Vincenzini (Ed.), High Tech Ceramics, Elsevier, Amsterdam, 1987, pp. 189–213.
[2] J.C. Elliott, Structure and Chemistry of the Apatites and Other Calcium Orthophosphates, Elsevier, Amsterdam, 1994.
[3] Y. Sun, G. Guo, D. Tao, Z. Wang, Reverse microemulsion-directed synthesis of hydroxyapatite nanoparticles under hydrothermal conditions, Journal of Physics and Chemistry of Solids 68 (2007) 373–377.
[4] Y. Wang, S. Zhang, K. Wei, N. Zhao, J. Chen, X. Wang, Hydrothermal synthesis of hydroxyapatite nanopowders using cationic surfactant as a template, Materials Letters 60 (2006) 1484–1487.
[5] H. Aoki, Science and Medical Application of Hydroxyapatite, Japanese Association of Apatite Science, Tokyo, Japan, 1991.
[6] R.Z. Legeros, Calcium Phosphates in Oral Biology and Medicine, Karger, Basel, Switzerland, 1991.
[7] C. Qiu, X. Xiao, R. Liu, Biomimetic synthesis of spherical nano-hydroxyapatite in the presence of polyethylene glycol, Ceramics International 34 (7) (2008) 1747.
[8] R. Murugan, S. Ramakrishna, Development of nanocomposites for bone grafting, Composites Science and Technology 65 (15–16) (2005) 2385–2406.
[9] M. Tanahashi, K. Kamiya, T. Suzuki, H. Nasu, Fibrous hydroxyapatite grown in the gel system: effects of pH of the solution on the growth rate and morphology, Journal of Materials Science Materials in Medicine 3 (1992) 48–53.
[10] R. Kumar, K.H. Prakash, K. Yennie, P. Cheang, K.A. Khor, Synthesis and characterization of hydroxyl apatite nano rods/whiskers, Key Engineering Materials 284–286 (2005) 59–62.
[11] K. Lin, J. Chang, R. Cheng, M. Ruan, Hydrothermal microemulsion synthesis of stoichiometric single crystal hydroxyapatite nanorods with mono-dispersion and narrow-size distribution, Materials Letters 61 (2007) 1683.
[12] Q.J. He, Z.L. Huang, Template-directed growth and characterization of flowerlike porous carbonated hydroxyapatite spheres, Crystal Research Technology 42 (5) (2007) 460–465.
[13] B. Prelot, T. Zemb, Calcium phosphate precipitation in catanionic templates, Materials Science Engineering C 25 (2005) 553–559.
[14] Y. Zhang, L. Zhou, D. Li, N. Xue, X. Xu, J. Li, Oriented nano-structured hydroxyapatite from the template, Chemical Physics Letters 376 (2003) 493–497.

[15] W.J. Shih, M.C. Wang, M.H. Hon, Morphology and crystallinity of the nanosized hydroxyapatite, synthesized by hydrolysis using cetyltrimethylammonium bromide (CTAB) as a surfactant, Journal of Crystal Growth 275 (2005) 2339–2344.
[16] Y. Sun, G. Guo, Z. Wang, H. Guo, Synthesis of single-crystal HAp nanorods, Ceramics International 32 (2006) 951–954.
[17] L. Yan, Y. Li, Z. Deng, J. Zhuang, X. Sun, Surfactant-assisted hydrothermal synthesis of hydroxyapatite nanorods, International Journal of Inorganic Materials 3 (2001) 633–637.
[18] M. Cao, Y. Wang, C. Guo, Y. Qi, C. Hu, Preparation of ultrahigh-aspect-ratio hydroxyapatite nanofibers in reverse micelles under hydrothermal conditions, Langmuir 20 (2004) 4784–4786.
[19] Y. Liu, D. Hou, G. Wang, A simple wet chemical synthesis and characterization of hydroxyapatite nanorods, Materials Chemistry and Physics 86 (2004) 69–73.
[20] D.W. Halcomb, R.A. Young (Eds.),Thermal decomposition of human tooth enamel and calcif Tissue International 31 (1980) 189.
[21] K. Ioku, M. Yoshimura, S. Munemiya (Eds.),Preparation of hydroxyapatite by hydrothermal reaction Nippon Kagaku Kaishi (1985) 1565–1572.
[22] B.O. Fowler, Structural properties of hydroxyapatite and related compound, Gaithersburg (1968).
[23] R.N. Panda, M.F. Hsieh, R.J. Chung, T.S. Chin, FTIR, XRD, SEM and solid state NMR investigations of carbonate-containing hydroxyapatite nano-particles synthesized by hydroxide-gel technique, Journal of Physics and Chemistry of Solids 64 (2003) 193–199.
[24] T.K. Anee, M. Ashok, M. Palanichamy, S. Narayana Kalkura, A novel technique to synthesize hydroxyapatite at low temperature, Materials Chemistry and Physics 80 (2003) 725–730.